Unconscious Learning versus Visual Perception: Dissociable Roles for Gamma Oscillations Revealed in MEG

Maximilien Chaumon[1], Denis Schwartz[2], and Catherine Tallon-Baudry[1,2]

Abstract

■ Oscillatory synchrony in the gamma band (30–120 Hz) has been involved in various cognitive functions including conscious perception and learning. Explicit memory encoding, in particular, relies on enhanced gamma oscillations. Does this finding extend to unconscious memory encoding? Can we dissociate gamma oscillations related to unconscious learning and to conscious perception? We investigate these issues in a magnetoencephalographic experiment using a modified version of the contextual cueing paradigm. In this visual search task, repeated presentation of search arrays triggers an unconscious spatial learning process that speeds reaction times but leaves conscious perception unaffected. In addition to a high-frequency perceptual gamma activity present throughout the experiment, we reveal the existence of a fronto-occipital network synchronized in the low gamma range specifically engaged in unconscious learning. This network shows up as soon as a display is searched for the second time and disappears as behavior gets affected. We suggest that oscillations in this network shape neural processing to build an efficient neural route for learned displays. Accordingly, in the last part of the experiment, evoked responses dissociate learned images at early latencies, suggesting that a sharpened representation is activated without resort on learning gamma oscillations, whereas perceptual gamma oscillations remain unaffected. ■

INTRODUCTION

Learning is considered to rely on the modification of synapses and pathways: Training progressively builds a more efficient neural route through the modification of neural connectivity (Hebb, 1949). The mechanisms of synaptic plasticity underlying learning are highly sensitive to the precise timing of neural activity (Abbott & Nelson, 2000; Bi & Poo, 1998; Markram, Lubke, Frotscher, & Sakmann, 1997) and are more likely to take place upon repeated stimulation. Because oscillatory synchrony offers an opportunity to control precisely the timing of pre- and postsynaptic activities and to repeat this precise temporal pattern at each oscillation cycle, it has long been suspected to be involved in learning and memory (Singer, 1995, 1999) and was recently observed during memory performance in animals in the hippocampal region (Bauer, Paz, & Pare, 2007; Montgomery & Buzsaki, 2007; Csicsvari, Jamieson, Wise, & Buzsaki, 2003; Bragin et al., 1995) and in the neocortex (Stiefel, Tennigkeit, & Singer, 2005; Rodriguez, Kallenbach, Singer, & Munk, 2004; Wespatat, Tennigkeit, & Singer, 2004).

Studies in humans suggest a role of induced gamma band (30–120 Hz, non-phase-locked to the stimulus) oscillations in coupling perception and learning (Jensen, Kaiser, & Lachaux, 2007). Memory encoding, under its simplest form, appears as a decrease (or sometimes increase) of neural activity upon repeated presentations of the same stimulus. This phenomenon, known as repetition suppression (Grill-Spector, Henson, & Martin, 2006), can be specifically observed in the gamma band (Gruber & Müller, 2002, 2005, 2006). Episodic memory encoding also seems to benefit from oscillatory synchrony: Enhanced gamma oscillations have been observed during the presentation of an item when it is subsequently remembered compared to when it is forgotten (Osipova et al., 2006; Gruber, Tsivilis, Montaldi, & Müller, 2004; Sederberg, Kahana, Howard, Donner, & Madsen, 2003; Fell et al., 2001). Last, higher levels of synchrony in the gamma band have also been observed in an operant conditioning task (Miltner, Braun, Arnold, Witte, & Taub, 1999) and in a paired associate learning task (Gruber, Keil, & Müller, 2001).

These findings raise two questions. First, is induced gamma activity only involved in the formation of explicit memories or can it also be observed during unconscious learning? Second, how can one relate the role of induced gamma oscillations in learning with its role in visual perception (Tallon-Baudry & Bertrand, 1999)? In

[1]Université Pierre et Marie Curie (Paris6), LENA CNRS UPR640, Paris, France, [2]MEG-EEG Center, Hôpital de la Pitié-Salpêtrière, Paris, France

other words, can we dissociate the induced gamma oscillations involved in establishing a coherent percept from those involved in learning and memory?

To investigate these issues, we used a task in which learning occurs but that leaves subjective perception intact in a magnetoencephalographic (MEG) experiment. We took advantage of the recently developed contextual cueing paradigm (Chun & Jiang, 1998), which probes specifically the unconscious learning of spatial relations between target and distractors in visual search, and proposed a modified version of this paradigm (Chaumon, Drouet, & Tallon-Baudry, 2008). Subjects searched and reported the orientation of a T-shaped target (tilted either 90° to the right or to the left) among L-shaped distractors. Unknown to the subject, there was only a limited number of distractor configurations that were all repeated several times throughout the experiment (Figure 1). Half of the distractor configurations were consistently associated with the same target position throughout the experiment. This set of displays defines the predictive (P) condition, in which the distractor configuration predicts the target position (e.g., display P1 on Figure 1B). The other half of distractor configurations were presented with different target positions from one repetition to the other and define the nonpredictive (nP) condition: In this case, the distractor layout does not allow predicting the target position (e.g., display nP1 on Figure 1B). This paradigm explicitly controls for repetition effects (Grill-Spector et al., 2006; Gruber & Müller, 2002): P and nP configurations are repeated the same number of times. After a few repetitions of all the configurations, subjects respond faster in the predictive than in the nonpredictive condition, showing that learning of target–distractor relations takes place. Importantly, subjective visual perception is not affected: Subjects do not discriminate the repeated displays from new ones, nor do they have any explicit knowledge of the layout–target relationships (Chaumon et al., 2008). This paradigm thus allows modulating performance by learning without modifying subjective perception. We monitored induced gamma band oscillations along the experiment to see whether we could dissociate unconscious learning and subjective perception in the gamma band.

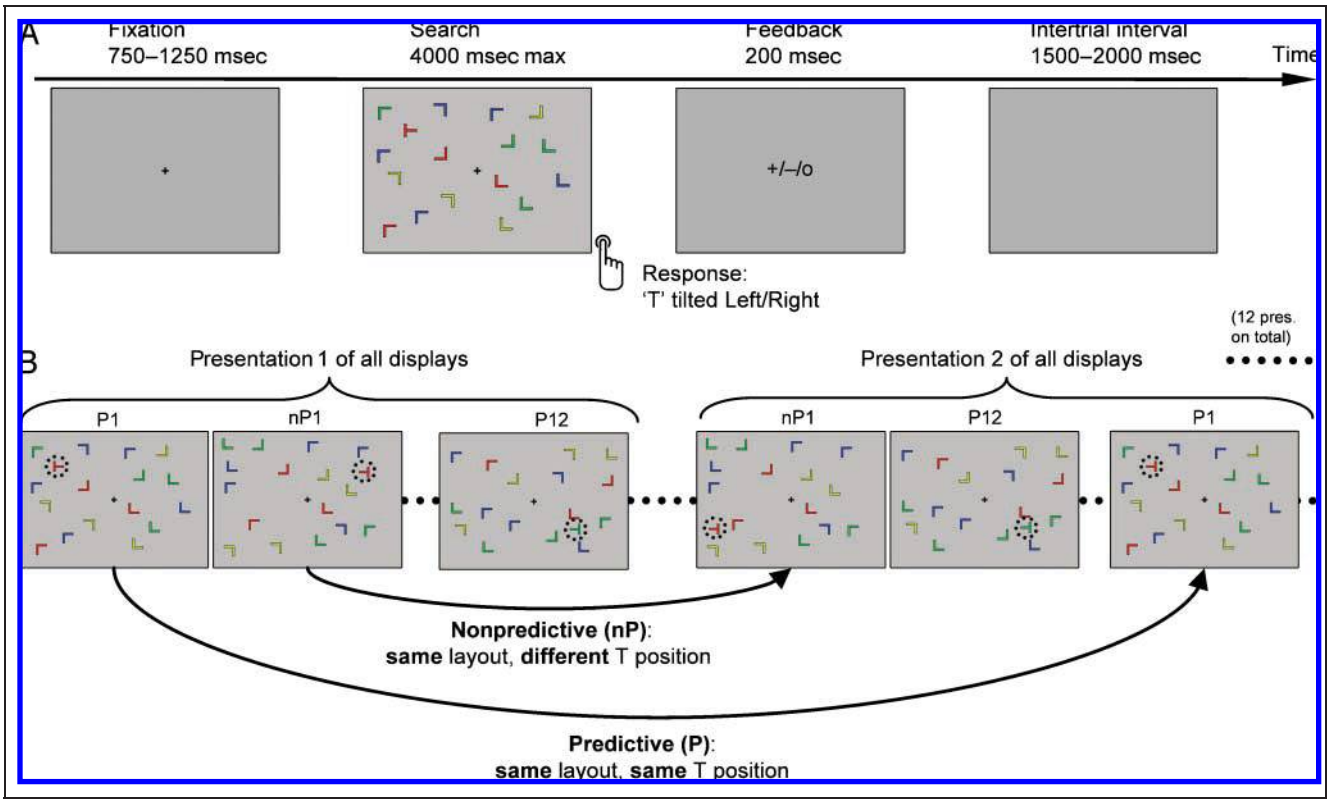

Figure 1. Paradigm. (A) Subjects searched for the ''T'' and reported its orientation (tilted left or right). The subject's response (around 1400 msec on average) interrupted the visual display and triggered a feedback screen (''+''or ''−'' for good and bad response, respectively). An absence of response after 4 sec was followed by an ''o'' feedback. Subjects were asked to avoid moving their eyes for half a second when the display appeared. (B) Experimental sequence. In the predictive (P) displays, a given array of distractors was associated with the same target position throughout the experiment (e.g., array P1 is associated here with a T in the upper left quadrant). In the nonpredictive (nP) displays, the target location changed on each presentation of a given array of distractors (e.g., array nP1 here). Subjects performed the task on 12 P and 12 nP configurations randomly intermingled for about half an hour. Another set of 12 P and 12 nP configurations was then generated and the task resumed for another half hour.

METHODS

Stimuli

Each display consisted of 17 colored (red, green, blue, or yellow) items (1 T target embedded in a unique configuration of 16 L distractors, 0.4° × 0.4° of visual angle) on a mid-gray background. ''L'' shapes were presented randomly in one of four orientations (0°, 90°, 180°, or 270°). Items were placed on an invisible 12 × 10 grid subtending 12.5° × 7.5° and allowed to jitter around their position by a maximum of 0.5°. This jitter was kept constant all along the experiment for a given configuration. Target positions were constrained to 12 possible locations arranged symmetrically with respect to the center of the screen. An L could never appear at any of these 12 locations. The number of items per quadrant varied from 3 to 5. A new set of stimuli was generated for each subject.

Paradigm

The time course of one trial is shown on Figure 1A. Each trial began with a fixation cross in the center of the screen for 750 to 1250 msec. The search array appeared at time zero and subjects were asked to find the T as quickly and as accurately as possible and report its orientation by two-choice button press. The subject's response (on average, around 1400 msec) interrupted the search display presentation and triggered a feedback screen (''+''or ''−'' for good or bad response, respectively) and initiated the next trial. If the subject did not respond within 4000 msec, an ''o'' sign indicated timeout and the next trial was initiated. The intertrial interval was 1500 to 2000 msec. Unknown to the subjects, images consisted in two randomly intermingled categories of displays.

Two sets of 24 images each were generated for each subject, presented 12 times each in random order. For the predictive set (P), images were repeated as is. All the elements of each image were exactly at the same position during the whole experiment (only the orientation of the T was changing to avoid simple stimulus–response learning and direct motor specification; Neumann & Klotz, 1994). Hence, in the P condition, each context (of Ls) predicted a specific position of the target (see, for instance, display P1 on Figure 1B). For the nonpredictive set (nP), images were also repeated but the position of the target changed from one presentation of an image to another. In this condition, each context was nonpredictive of the position of the target (display nP1 on Figure 1B). This paradigm extends contextual cueing by controlling explicitly for repetition effects (Grill-Spector et al., 2006). Indeed, whereas in the original contextual cueing paradigm only the displays that were learned were repeated, all images from the two conditions are repeated the same number of times in the present experiment.

New sets of P and nP configurations were generated for each subject and presented 12 times. The 12 possible target locations were used the same amount of times across repetitions in both the P and nP conditions. Twelve P and 12 nP configurations were presented 12 times in the first half of the experiment (Runs 1 to 3) and another 12 P and 12 nP configurations was presented for the second half of the experiment (Runs 4 to 6).

The two types of configurations were randomly intermixed in an unpredictable manner for each subject with the constraint that the number of intervening items between two successive occurrences of the same image was similar in the P and nP configurations (mean and standard deviation differing by less than 5% for each subject). Subjects were not informed in any way of the structure of the task.

Procedure

Sixteen healthy adult volunteers (mean age = 25 years, range = 19–31 years, 8 men, 14 right-handed) performed the task while their brain activity was monitored using MEG. All gave their written informed consent and were paid for their participation, according to procedures approved by the national ethics committee (CCPPRB no. 0233). Subjects were familiarized with the task by a practice block of 48 trials. Images were back-projected onto a translucent screen disposed at 110 cm using a computer data projector (60 Hz) and the Psychophysics Toolbox extension for MATLAB (www.psychtoolbox.org/) (Brainard, 1997). The experiment was divided in 6 runs of 96 trials (4 presentations of each image), lasting about 8 min each. Runs 1 to 3 were performed on the first half of the stimuli (12 P and 12 nP) and Runs 4 to 6 on the other half (remaining 12 P and 12 nP). The responding hand was switched in the middle of the experiment. The subjects' head position was monitored and no deviation larger than 0.5 cm allowed. After the six runs, subjects were first asked to report anything they noticed about the displays during the experiment. If they did not mention that displays were repeated, they were then asked explicitly whether they noticed any repetition during the experiment. Finally, the subjects were informed about the existence of the repeated P and nP configurations, and performed a series of behavioural tests to check whether the knowledge acquired implicitly could be used explicitly.

Recordings

Continuous data were collected at the MEG–EEG Centre, Hôpital Pitié-Salpêtrière (Paris, France) using a CTF/VSM OMEGA 151-channels third-order gradiometer, whole-head system (CTF Systems, Vancouver, Canada) at a sampling rate of 1250 Hz, together with the electrocardiogram, as well as vertical and horizontal electrooculograms (EOG). Cardiac artifacts picked up in the MEG

signal were corrected by a correlation method (Gratton, Coles, & Donchin, 1983). The EOG was calibrated for each subject and the rejection threshold was set to 1°. Trials contaminated with muscle artifact (visual inspection) were also rejected. The window of analysis ranged from 400 msec prior to stimulus onset to 400 msec after. This relatively narrow time window was the best compromise between having a long enough poststimulus epoch and not rejecting too many trials. Subjects were explicitly asked to avoid making saccades for half a second after the display appeared. On average, 59.0 trials ± 0.8 *SEM* were included in each four presentations phase after artifact correction.

Data Analysis: Induced Oscillatory Power Measures

A wavelet transform was applied to each trial (−600 to 700 msec around search array onset) at each sensor, using complex Morlet wavelets characterized by the ratio $f_0/\sigma f = 8$ (Tallon-Baudry, Bertrand, Delpuech, & Pernier, 1996), resulting in an estimate of power at each sample in time and at each frequency (2 Hz step) between 10 and 120 Hz. The resulting time–frequency data were then averaged across trials for P and nP configurations for Presentations 2 to 5 and 9 to 12 separately. As explained in the Results section, these periods were devised from the behavioral data. This strategy led us to skip Presentations 6 to 8. Indeed, the data are presented in periods of four presentations in order to keep a constant and relatively low signal-to-noise ratio (precluding the use of the 6 to 8 period, which includes 25% fewer trials than the other periods). We also wanted to avoid any overlap between periods, and thus, did not include the 6 to 9 period in the analysis because it overlaps with the 9 to 12 period (but see Supplementary Figure 1). For statistical comparison, data were averaged on time–frequency windows of interest (as mentioned each time in the results section), divided by the corresponding baseline activity (same frequency range, 300 to 100 msec before stimulus onset), and log transformed to approach a normal distribution prior to performing statistical analysis (Kiebel, Tallon-Baudry, & Friston, 2005). Henceforth, any mention of spectral power refers to the log-transformed data. For each measure, the baseline activity was measured in the same frequency band but in the baseline time window and was never different across conditions (paired t tests, all $p > .15$) except for the perceptual gamma response (54–120 Hz, Presentations 2–5, $p = .06$, as detailed in the Results section). Data preprocessing and wavelet analysis were performed using in-house software.

Data Analysis: Long-range Synchrony

Synchrony analysis was performed following the procedure suggested by Lachaux, Rodriguez, Martinerie, and Varela (1999), which provides a method of measuring synchronous oscillatory activity independent of the signal's amplitude. For each subject, at each time t and frequency f, the result of the convolution for trial j is a complex number $A_j(t,f)e^{i\varphi_j(t,f)}$, where A represents the amplitude of the signal and φ represents its phase. Phase-locking ρ_{kl} between sensors k and l is computed in the time–frequency domain across N single trials as follows:

$$\rho_{kl} = \left| \frac{1}{N} \sum_{j=1}^{N} e^{i(\varphi_{jk}(t,f) - \varphi_{jl}(t,f))} \right|$$

Phase-locking values were computed on all pairs of electrodes between the two pools used for power measures between 30 and 48 Hz, between 100 and 400 msec (209 pairs between the electrodes highlighted on Figure 3B, top). The phase-locking values were then averaged across trials, frequencies, time, and pairs. The phase-locking value during baseline was subtracted and the results were compared between conditions by means of nonparametric Wilcoxon signed-rank tests. Baseline was taken from −400 to −100 msec (instead of −300 to −100 msec in the power analysis) in order to equate the number of time samples between poststimulus and baseline windows. Baseline synchrony was systematically compared between conditions and Wilcoxon signed-rank tests for matched pairs showed no significant difference between P and nP baseline synchrony (all $p > .1$).

RESULTS

Learning Contextual Associations: Behavior

Reaction times decreased with practice for all configurations but were further shortened on predictive (P) configurations after just five presentations. Figure 2A shows the average reaction times of the subjects across presentations. Behavioral facilitation occurs from the sixth presentation on (Figure 2A and Supplementary Table 1). Therefore, we define two phases in the remainder of the article: a learning phase, before behavioral facilitation (Presentations 2 to 5; Presentation 1 is excluded from the analysis because images are neither predictive nor nonpredictive as none has been seen before) and an exploiting phase at the end of the experiment, when the behavioral facilitation is firmly established (Presentations 9 to 12). Figure 2B summarizes the behavioral results for the learning and exploiting phases. In the learning phase, reaction times did not differ between P and nP configurations [paired t test, $t(15) = 0.12, p > .9$], while at the end of the experiment (Presentations 9 to 12), reaction times on P configurations were shortened compared to nP configurations [paired t test, $t(15) = 4.87, p < .001$]. Average error rates were low (2.6 ± 0.7%)

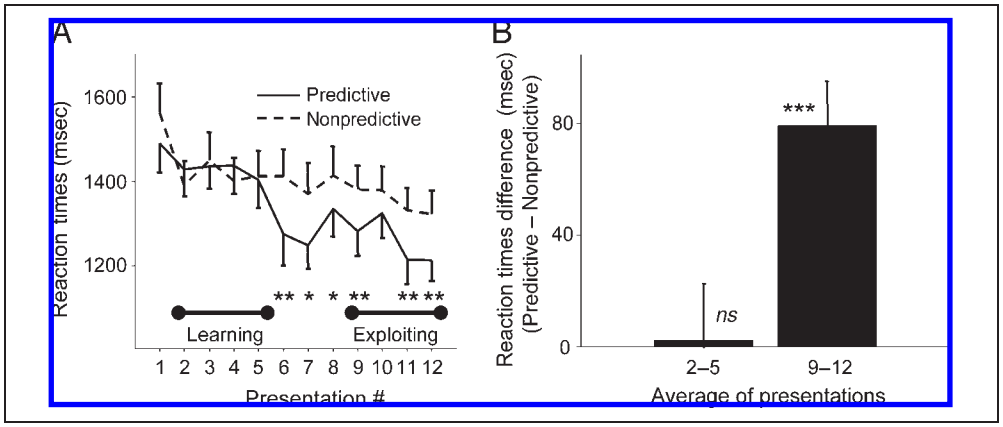

Figure 2. Behavioral results. (A) Average reaction times across subjects as a function of presentation number. (B) Average contextual cueing effect (predictive minus nonpredictive reaction times) across subjects averaged during the learning phase (Presentations 2 to 5) and during the exploiting phase (Presentations 9 to 12). Level of significance of the paired *t* tests: $*p < .05$, $**p < .01$, $***p < .001$. The error bars show the standard error of the mean.

and did not differ between conditions [paired *t* test, $t(15) = 0.80, p > .4$].

Importantly, subjective visual perception was not altered by learning. As detailed in a previous article (Chaumon et al., 2008), all the subjects went through a debriefing questionnaire during which none of them reported having noticed any repetition. No subject reported trying to remember the displays or any spatial property of the displays. The learning of the spatial context–target associations was thus implicit in this experiment. In addition, subjects were submitted to three postexperimental tests meant to assess specifically the form of knowledge required for the behavioral facilitation. The first test was designed to identify potential traces of familiarity with the identity of the visual displays. A nonspeeded two-alternative forced-choice (2AFC) old/new test was used: Subjects were presented with two different configurations and had to decide which one had been seen before (the other being a new one never presented before). The two next tests were designed to reveal explicit knowledge of the target location in a given context. Because these tests probed the spatial knowledge acquired and used in the experiment, they could be more sensitive than the familiarity test of the first old/new test (Chun & Jiang, 2003). In one test, we presented the subjects with predictive configurations of distractors seen during the experiment, but without any target (the target position was unoccupied, only the 16 distractors were present in the image), and asked them to decide in which quadrant the target should have been (4AFC). Finally, subjects saw predictive configurations in which a second target was added (in the opposite quadrant from that of the target), and were asked to choose which one was at the correct location (2AFC). In this test, in addition to the type of knowledge, we matched the task settings to those of the actual experiment. Before responding, subjects had to perform a visual search task, as they did during the MEG recordings. In all these three tests, however, the group of subjects did not show any reliable sign of explicit memory of the spatial structure of the displays (Kolmogorov–Smirnoff test against a binomial distribution, all $p > .1$). Subjects were thus able to use their memory of spatial regularities to speed visual search, but were at chance when it came to using this knowledge explicitly (but see Smyth & Shanks, 2008).

A Specific Gamma Activity during Unconscious Learning

Our first goal in this experiment was to investigate whether a neural correlate of the unconscious learning of contextual associations could be found in the gamma band. We thus looked for an induced gamma activity that differentiates P from nP displays during the learning phase of the experiment (Presentations 2 to 5). The largest difference between P and nP responses during the learning phase peaked in the 30–48 Hz band, between 100 and 400 msec. Sensors with the highest amplitude difference (above 0.05 power change relative to baseline in log units) between conditions in this window defined regions of interest (highlighted with black and white disks on the map; Figure 3B). A left occipito-temporal region and a frontal region appeared in this manner. One exemplar sensor from each region is shown on Figure 3A.

The occipital learning effect corresponds to an increase in gamma band oscillations in response to P displays during learning specifically, as shown on the maps of Figure 3C. Figure 3D shows the average of this gamma activity on the left occipito-temporal cluster. During the learning phase, the mean 30–48 Hz, 100–400 msec power is significantly larger in the P than in the nP condition [paired *t* test, $t(15) = 3.6, p < .005$]. This activity is present in response to P displays only: Comparing directly the mean 30–48 Hz, 100–400 msec power with baseline reveals the existence of a significant response in the P condition only [Presentations 2–5, paired *t* test against baseline, P condition: $t(15) = 2.6, p < .05$; nP condition: $t(15) = -0.1, p > .5$]. Importantly, this left occipito-temporal gamma activity is not present any longer during the exploiting phase [paired *t* test against

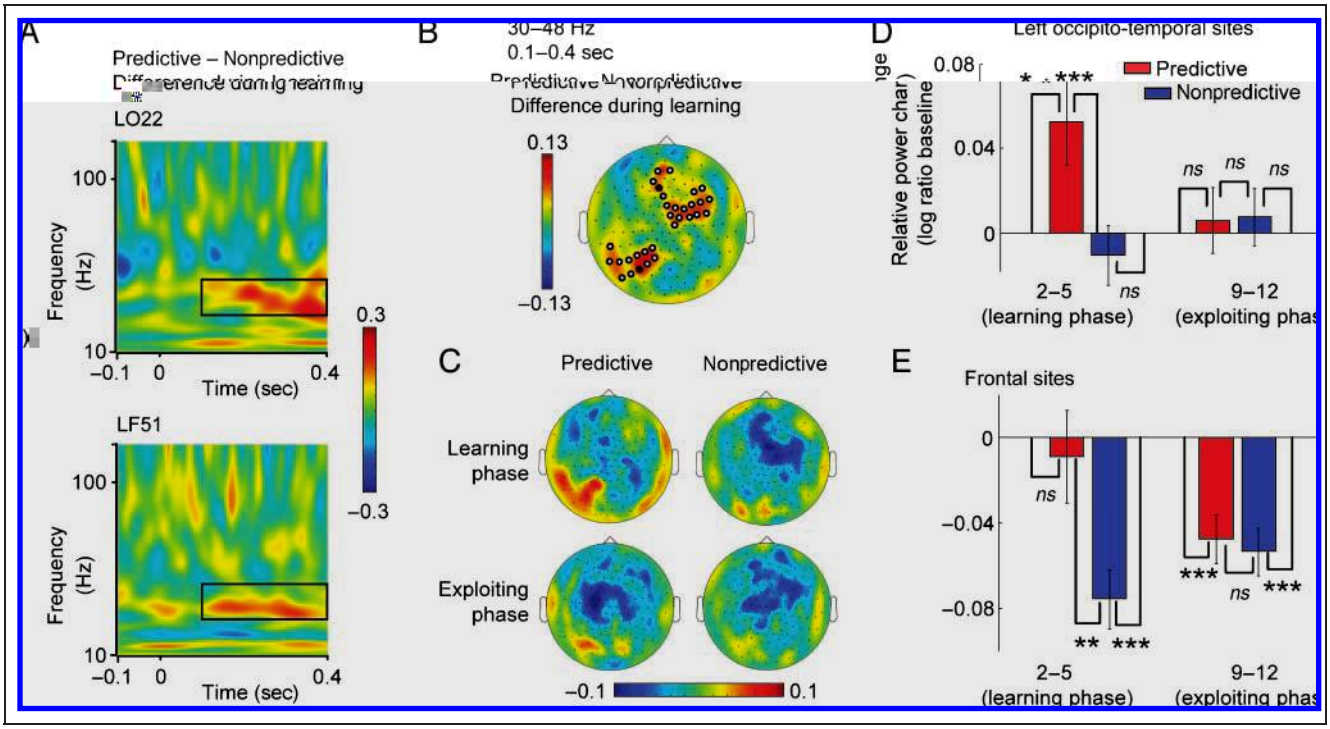

Figure 3. Specific learning activities in the gamma band. Gamma modulations in the 100–400 msec, 30–48 Hz time–frequency (TF) window occurred during the learning phase specifically. (A) TF plots showing the difference between responses to predictive (P) and nonpredictive (nP) displays during learning at a frontal (LF51, top) and an occipital (LO22, bottom) sensor (black dots on the map in B). The black boxes in these TF plots highlight the 30–48 Hz, 100–400 msec window of interest used for the rest of the figure. (B) Topography of the difference in the TF window of interest, revealing a left occipito-temporal and a frontal cluster. (C) Topographical maps of the mean 30–48 Hz, 100–400 msec gamma activity during learning, separately in the P and nP conditions. (D) Average activity on the sensors highlighted at left occipito-temporal sites in B. Gamma activity is specifically increased in the P condition during learning. (E) Average activity on the sensors highlighted at frontal sites in B. Gamma activity at frontal sensors is decreased in the nP condition during learning. Data on all plots and maps show the log ratio of power change in the TF windows of interest relative to baseline. Level of significance of the paired *t* tests: $*p < .05$, $**p < .01$, $***p < .001$, *ns* = nonsignificant.

baseline, P condition: $t(15) = 0.4$, $p > .5$; nP condition: $t(15) = 0.6$, $p > .5$; paired t test P vs. nP: $t(15) = 0.1$, $p > .8$].

A more thorough exploration of the development of this learning-specific occipital activity is shown on Figure 4A. Initially, on the first presentation, left occipito-temporal gamma activity is low and identical in the P and nP conditions. Upon start of the second presentation, left occipito-temporal gamma activity in the P condition rises sharply and is maintained at a high level until Presentation 5. This left occipito-temporal activity then drops abruptly on Presentation 6, when reaction times begin to be significantly shortened (Supplementary Table 1). Supplementary Table 2 shows the numerical values of the statistical comparison at each presentation and confirms this observation despite the small number of trials at each presentation (14.8 trials ± 1.0 *SEM*). This result shows that the learning activity is purely specific to the learning phase and is not present after Presentation 5. It could have been that the difference in activity persists on the next presentations but at a different frequency. We have checked that this is not the case and show on Supplementary Figure 1 that no differential gamma activity is present during Presentations 6 to 9 and 9 to 12, even at other frequencies. In sum, a left occipito-temporal gamma activity in the 30–48 Hz range is specific of unconscious learning: It is present only during the learning phase in response to the P displays and disappears abruptly at the onset of the behavioral effect.

The pattern of results over frontal sites is quite different. Activity at these sites is generally below baseline level. The basic reaction to the presentation of an image at these sites thus seems to be a suppression of gamma activity, except in the P condition during learning, as shown on the maps of Figure 3C. The bar plot of Figure 3E shows the average activity of the frontal cluster. During the exploiting phase, measures show an equivalent suppression of gamma activity: Both P and nP displays trigger a significant decrease relative to baseline [paired t test against baseline, Presentations 9–12, P condition: $t(15) = 4.3$, $p < .001$; nP condition: $t(15) = 4.8$, $p < .0005$] but are not different from each other [paired t test, P vs. nP: $t(15) = 0.5$, $p > .5$; see also Supplementary Figure 1 for similar results during Presentations 6 to 9]. During the learning phase, a dissociation between P and nP displays seems to act in addition to this suppression. P and nP responses are different [paired t test,

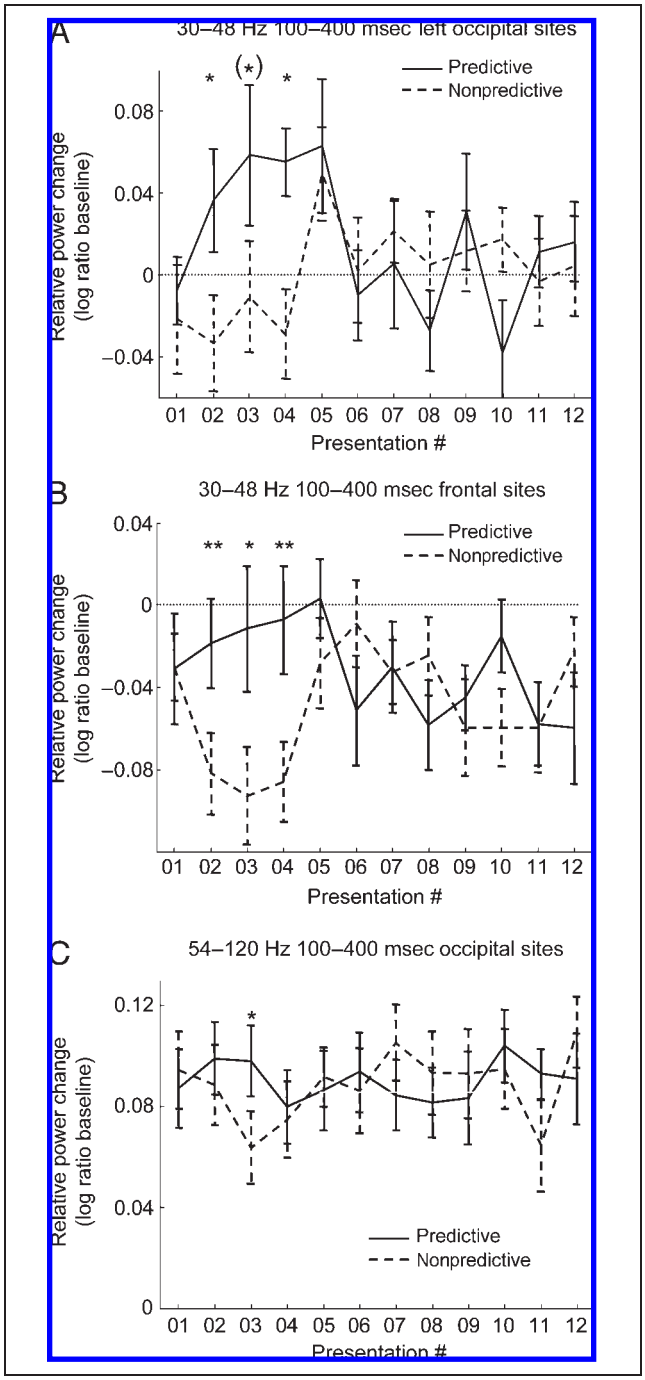

Figure 4. The learning gamma activity dissociates predictive (P) and nonpredictive (nP) displays after a single presentation. Presentation by presentation breakdown of the learning-related and perceptual gamma activities. In the 30–48 Hz, 100–400 msec time–frequency (TF) window, gamma activity at left occipito-temporal (A) and frontal (B) sites dissociates P and nP conditions during learning and disappears afterward. On the other hand, in the 54–120 Hz, 100–400 msec TF window at occipital sites (C), gamma activity is relatively high in both conditions during the whole experiment. Level of significance of the paired t tests: $*p < .05$, $**p < .01$.

$t(15) = 3.2, p < .01$], the response to nP displays is below baseline [paired t test against baseline, $t(15) = 5.5$, $p < .0001$], whereas the response to P displays is not [paired t test against baseline, $t(15) = 0.4, p > .6$].

A more thorough examination of Figure 4B confirms the specificity of the dissociation during learning. Initially, on the first presentation, frontal gamma oscillations are identical in the P and nP conditions. Upon start of the second presentation, a sharp decrease occurs in the nP condition which holds for three presentations. During this period, activity in the P condition gradually increases toward baseline level. Activity then returns to a similar level in the P and nP conditions from Presentation 5 onward, just one presentation before reaction times begin to be significantly shortened in the P condition (Figure 2A). Supplementary Table 2 shows the numerical values of the statistical comparison between P and nP responses in the gamma band at each presentation. This result shows that the dissociation between conditions is purely specific to the learning phase and is not present after Presentation 5. It could have been that the difference in activity persists on the next presentations but at a different frequency. We have checked that this is not the case and show on Supplementary Figure 1 that no differential gamma activity is present during Presentations 6 to 9 and 9 to 12, even at other frequencies. In sum, gamma activity in the 30–48 Hz is decreased at frontal sites during the whole experiment and nP displays trigger an additional suppression of activity in the 30–48 Hz frequency range specific to the learning phase.

Are the left occipito-temporal gamma increase and the frontal gamma decrease functionally related? As shown in Figure 4A and B, these two modulations occur on the same presentations, during the learning phase of the experiment. To address this issue, we analyzed long-range phase synchrony between these two regions. We computed phase synchrony across all pairs of sensors from the left occipito-temporal to the frontal regions, using the same sensors of interest as for power analysis between 30 and 48 Hz (inset Figure 5). We then averaged phase-locking values across the 209 pairs for each subject and experimental conditions, and compared the value obtained in the 100–400 msec time range with baseline value (Figure 5). During learning, synchrony between left occipito-temporal and frontal sensors was enhanced compared to baseline in the P condition, but decreased compared to baseline in the nP condition (Wilcoxon signed-rank test against baseline, P condition: $z = -2.8, p < .01$; nP condition: $z = -2.4, p < .05$). The direct comparison between the baseline-subtracted values in the P and nP conditions reveals a highly significant difference (Wilcoxon signed-rank test for matched pairs: $z = -3.5, p < .001$). This pattern of results lingers until the end of the experiment: The difference between conditions remains significant (P vs. nP baseline-subtracted synchrony values, Presentations 9–12, Wilcoxon

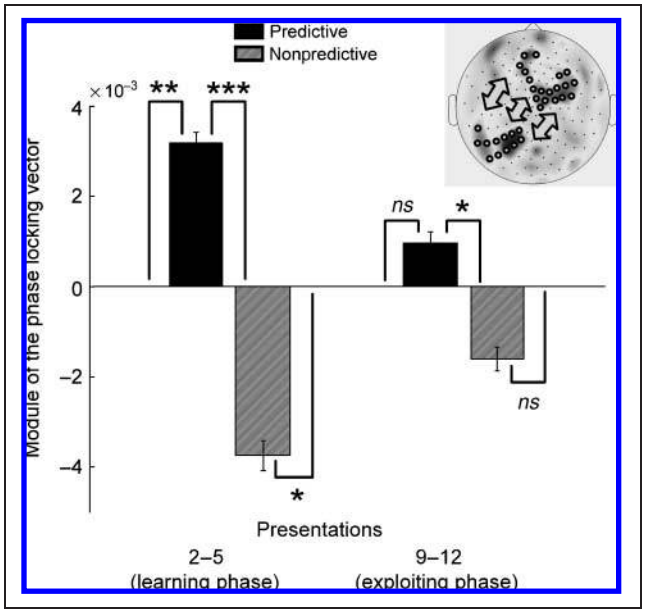

Figure 5. Frontal and left occipito-temporal sensors synchronize during learning. Long-range phase synchronization of electrode pairs from the two groups shown in the inset (sensors used in Figure 3) in the 30–48 Hz, 100–400 msec time–frequency window. Baseline subtracted phase-locking values show enhanced synchrony in the predictive condition and reduced synchrony in the nonpredictive condition during learning compared to baseline. This pattern of synchrony strongly decreases during the exploiting phase. Level of significance of the paired *t* tests: **p* < .05, ***p* < .01, ****p* < .001, *ns* = nonsignificant.

signed-rank test for matched pairs: $z = -2.3$, $p < .05$), but synchrony does not differ from baseline any longer, neither in the P nor in the nP condition (Wilcoxon signed-rank test against baseline, P condition: $z = -1.0$, $p > .3$ and nP condition: $z = -1.5$, $p > .1$).

Perceptual Gamma Response

We have identified a left occipito-temporal gamma response present only during the learning of context–target relations in the low gamma band (30–48 Hz). Both the topography and frequency range of this activity are quite different from the typical gamma response observed in response to any visual stimulus. A gamma response to a visual display is typically observed over midline occipital sites (Vidal, Chaumon, O'Regan, & Tallon-Baudry, 2006; Kaiser, Buhler, & Lutzenberger, 2004) and was shown to originate from the calcarine sulcus (Hoogenboom, Schoffelen, Oostenveld, Parkes, & Fries, 2006). We averaged power across all presentations in both experimental conditions to obtain an unbiased estimate of the maximal gamma response in our experiment (Fiebach, Gruber, & Supp, 2005). The sensor showing the maximal gamma response is located near the midline in the occipital region (sensor RO11; Figure 6A), and the topography of the mean 54–120 Hz, 100–400 msec is centered over posterior cortices (Figure 6B). This gamma response is present whenever a stimulus is delivered (Figure 6C), and we thus labeled it the perceptual gamma response. It is significantly different from baseline regardless of the experimental condition or the presentation rank (mean 54–120 Hz, 100–400 msec over the posterior sensors highlighted in Figure 6B, paired *t* tests against baseline, all $p < .00001$). This gamma response is thus quite different from the learning-related gamma activity, in frequency (30–48 Hz for learning, 54–120 Hz for perception), in topography (left occipito-temporal for learning, midline occipito-parietal for perception), and functionally (during the learning phase for learning, present throughout the experiment for perception).

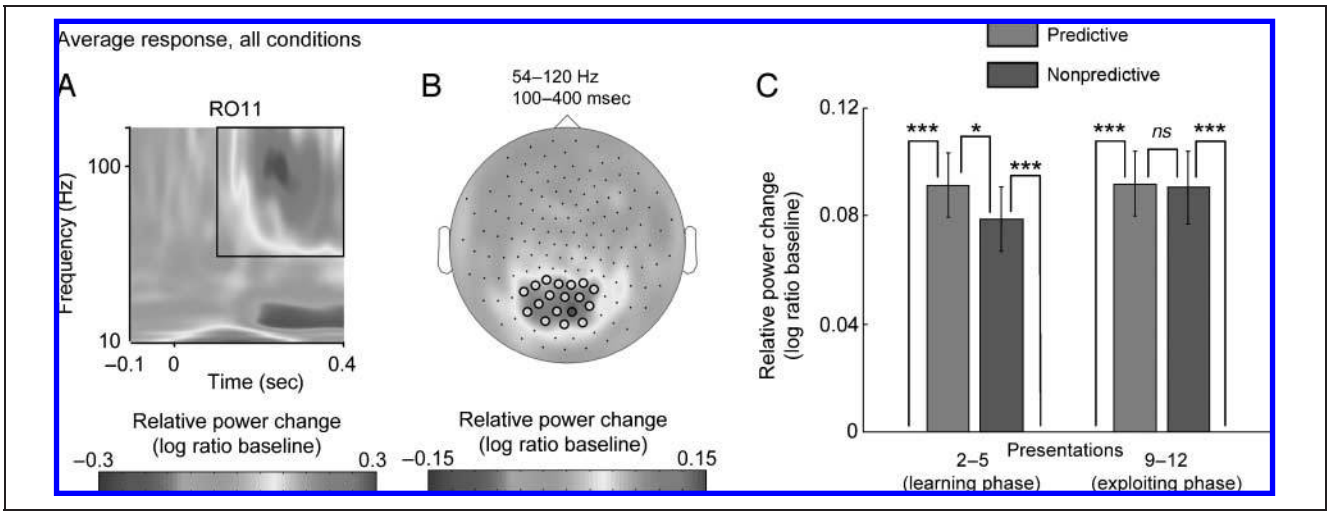

Figure 6. A perceptual gamma activity is present in all conditions. The maximal gamma response is seen at occipital sensors and little affected by learning. (A) Time–frequency (TF) plot at the most responding sensor (RO11) in the gamma band. (B) The response in the 54–120 Hz, 100–400 msec TF window is localized over medial occipital sensors. (C) The response in this TF window is present throughout the experiment, although slightly diminished in the nonpredictive condition during learning. Level of significance of the paired *t* tests: **p* < .05, ****p* < .001, *ns* = nonsignificant.

Importantly, the perceptual gamma response does not differentiate between P and nP conditions at the end of the experiment [Presentations 9–12, paired t test P vs. nP: $t(15) = 0.17$, $p > .8$], when it was checked that the subjects' conscious perception of P and nP displays did not differ. However, the perceptual gamma response appears to be slightly reduced in response to nP displays during the learning phase [Presentations 2–5, paired t test P vs. nP: $t(15) = 2.9$, $p < .05$]. However, part of this effect could be explained by the a nonsignificant trend in baseline signal [Presentations 2–5, paired t test P vs. nP during baseline: $t(15) = 1.99$, $p = .06$]. In sharp contrast with the learning-related activity which differs significantly between conditions during three consecutive presentations, the perceptual gamma response is different during Presentation 3 only (Figure 4C and Supplementary Table 3). The reduction shown in this perceptual response during the learning phase thus needs to be taken with caution.

In sum, we describe here an occipital gamma response that is present whenever a stimulus is presented, and may hence be related to perceptual processes rather than learning per se. Importantly, this perceptual gamma response is identical for P and nP displays at the end of the experiment, as is subjective perception, despite the marked behavioral advantage for P displays.

DISCUSSION

This experiment was designed to investigate whether and how gamma oscillations participate in the unconscious learning of contextual relations. We specifically asked whether unconscious learning would trigger gamma oscillations, and whether these learning-related oscillations would be different from the perceptual gamma response. Using a new version of the contextual cueing paradigm (Chun & Jiang, 1998) in MEG, we reveal a specific pattern of gamma activity at 30–48 Hz present over left occipito-temporal and frontal sites during the learning phase only. This learning-related activity co-occurs with a perceptual gamma activity at a higher frequency over midline occipito-parietal sensors, present in all conditions and throughout the experiment, whenever a visual display is presented. This perceptual activity does not differentiate between P and nP displays at the end of the experiment, when it was tested that subjects could not explicitly distinguish between the two types of displays.

We thus identified a perceptual gamma response and a learning-related gamma activity: Different gamma activities subserving different cognitive operations can thus be isolated in a single task (Wyart & Tallon-Baudry, 2008; Vidal et al., 2006). In addition, we reveal the existence of a fronto-occipital network synchronized in the low gamma range, specifically engaged in unconscious learning. This network is recruited as early as the start of the second display presentation, and is strongly activated before the onset of the behavioral effect. This suggests that this network shapes neural processing of the P displays, ultimately leading to a more efficient sharpened visual representation of context–target spatial relations. Once unconscious memories are formed, both neural processing times and reaction times get shorter. We suggest that the 30–48 Hz gamma activity triggers the neural plasticity necessary for the learning of context–target associations without the need for the subjects to become aware of these regularities.

A Fronto-occipital Synchronized Network Controls the Learning of Unconscious Context–Target Associations

The 30–48 Hz gamma increase seen here over left occipito-temporal sites is present only in the early phase of the experiment, when regular context–target associations are being learned and before behavior gets facilitated in the P condition. Gamma oscillations are thought to reflect the precise synchronization of neural activity across distributed cell assemblies and may participate in learning (Singer, 1995, 1999) through spike timing-dependent plasticity (Sejnowski & Paulsen, 2006; Bi & Rubin, 2005; Dan & Poo, 2004; Abbott & Nelson, 2000). As mentioned in the Introduction, several studies have previously shown the implication of gamma activity in explicit memory in humans (Sederberg et al., 2003, 2007; Osipova et al., 2006; Gruber et al., 2004; Fell et al., 2001). Because in contextual cueing, learning is unconscious (Chaumon et al., 2008; Chun & Jiang, 2003), the present results extend the role of gamma oscillations to unconscious learning.

Spatial learning usually activates right-lateralized brain structures. The left lateralization of the learning gamma activity observed here may thus seem surprising at first. However, left-lateralized learning-related gamma activity has been found for object learning (Supp, Schlögl, Trujillo-Barreto, Müller, & Gruber, 2007; Gruber, Trujillo-Barreto, Giabbiconi, Valdes-Sosa, & Müller, 2006). Left-lateralized activities in the hippocampus have also been reported in humans required to learn relational information between context and target objects (Ross & Slotnick, 2008; Greene, Gross, Elsinger, & Rao, 2007; Burgess, Maguire, & O'Keefe, 2002).

At frontal sites, the visual search displays trigger a decrease relative to baseline. This result was unexpected and its interpretation is uncertain. One possibility is that this decrease actually reflects the termination of an activity occurring before stimulus onset. Such expectation-related gamma activity present before stimulus onset at frontal sites has been observed previously (Summerfield & Mangels, 2006; Gonzalez Andino, Michel, Thut, Landis, & Grave de Peralta, 2005; Miltner et al., 1999). This activity would set the baseline level to a relatively high level and the apparent decrease after stimulus onset would actually be related to its termination. In addition,

frontal activity in the same frequency band dissociates P and nP displays during the learning phase. According to whether learning the target position relative to its context is advantageous (P condition) or deleterious (nP condition), this dissociation may reflect a frontal regulation of the flow of information through the temporal lobe (Miller & Cohen, 2001).

The pattern of long-distance synchronization is in striking agreement with this view: Frontal and left occipito-temporal sites get phase-synchronized in the P condition and desynchronized in the nP condition. We thus suggest that the underlying areas are part of a common network involved in the learning of new context–target associations. Because this regulation occurs unconsciously, this finding supports the hypothesis that the executive system can be recruited unconsciously (Lau & Passingham, 2007; Rose, Haider, & Büchel, 2005).

Frontal and Occipito-temporal Gamma Disappear When Learning Affects Behavior

The learning-related gamma modulations disappear as behavior gets facilitated in the P condition. It was suggested by Gruber and Müller (2002, 2005) that gamma oscillations may participate in the sharpening of neural representations. In this view, a new stimulus would elicit distributed processes coordinated by gamma oscillatory synchrony. Upon repeated presentations, the synaptic plasticity fostered by gamma oscillations (Wespatat et al., 2004) would help selecting the most relevant processes and lead to the creation of a sparser and faster neural route, resulting in a sharpened representation of the learned stimulus (Wiggs & Martin, 1998; Desimone, 1996). Indeed, we have previously shown using the same paradigm (Chaumon et al., 2008) that at the end of the experiment, event-related potentials differentiate between the P and nP conditions at surprisingly early latencies, between 50 and 100 msec, suggesting that learning has shaped a faster neural route for P displays.

It should be noted that the disappearance of the differential 30–48 Hz gamma activity also coincides with the end of an experimental run, just after the fourth presentation of all displays, when subjects were given a mandatory break of 2 min. The disappearance of the differential 30–48 Hz gamma activity might be related to a consolidation and sharpening process occurring during this 2-min rest period. This transition triggers transient changes in activity on the subsequent presentation which quickly stabilize after Presentation 6. This transition is intriguing and would deserve an accurate description. However, the low signal-to-noise ratio (due to the small number of trials at each presentation) requires us to describe differences in the signal that last for a few presentations (like the differences observed during the learning phase). On the other hand, the differential synchronization between frontal and occipital sensors, however, seems to last until the end of the experiment. This suggests that some learning processes still occur differently in the two conditions at this frequency.

An Efficient Learning Mechanism

The learning-related gamma activity is triggered as soon as the second presentation of the displays started. This result is highly surprising and has two implications: First, a memory trace of each display is formed on the first presentation and persists through at least 24 intervening trials (the average lag between two successive presentations of a given image). Second, information diagnostic of the predictive or nonpredictive nature of the image is extracted and matched against the memory trace on each encounter with a given image. Unconscious memory can store an impressive number of items (Jiang, Song, & Rigas, 2005) in just a few presentations. A highly efficient mechanism is thus at work to extract and use sufficiently detailed information to distinguish P and nP displays within the 100–150 msec necessary to trigger the learning gamma observed here. Our results agree with the idea that a rapid initial implicit processing stage carries this information and can initiate learning. The ''vision at a glance'' (Hochstein & Ahissar, 2002), sometimes referred to as the gist (Oliva, 2005), contains relevant information for the identification of scenes (Bar et al., 2006; Bar, 2004; VanRullen, 2003; Oliva & Schyns, 1997) and may enable shaping sensory processing according to task demands through feedback from high-order areas (Ahissar & Hochstein, 2004).

Multiplexing Different Functions at Distinct Frequencies

We identified two distinct components in the gamma range: a learning related activity, present only in response to P displays during the learning phase, and a perceptual gamma response, present in response to all stimuli throughout the experiment. Interestingly, neither the subject's conscious report nor the perceptual gamma response did differentiate between P and nP displays at the end of the experiment, suggesting that the perceptual midline occipito-parietal gamma response might be related here to subjective conscious perception. The mild suppression of the perceptual gamma response in the nP condition during learning might reflect an unconscious modulation of overall attentional allocation to these stimuli (although this result should be taken with caution, as explained in the Results section). Because attention is known to enhance memory encoding, this suppression may reflect an unconscious inhibition of memory encoding in the nP condition. The perceptual and learning-related gamma activities differed not only in terms of functional modulations but also in terms of frequency (high vs. low gamma range) and topography (midline occipito-parietal vs. left occipito-temporal).

These results add further support to the idea that distinct neural networks can synchronize their activity at different frequencies within the gamma range to subserve distinct cognitive processes (Wyart & Tallon-Baudry, 2008; Vidal et al., 2006). Gamma band oscillations have been related to a variety of cognitive functions: visual grouping (Kaiser et al., 2004; Tallon-Baudry et al., 1996), attentional bottom–up and top–down selection (Wyart & Tallon-Baudry, 2008; Herrmann, Munk, & Engel, 2004; Fries, Reynolds, Rorie, & Desimone, 2001; Gruber, Müller, Keil, & Elbert, 1999; Tallon-Baudry, Bertrand, Delpuech, & Pernier, 1997), short- (Tallon-Baudry, Bertrand, & Fischer, 2001) and long-term (Sederberg et al., 2003, 2007; Osipova et al., 2006; Gruber et al., 2004; Fell et al., 2001; Miltner et al., 1999) memory, as well as awareness (Wyart & Tallon-Baudry, 2008; Melloni et al., 2007; Schurger, Cowey, & Tallon-Baudry, 2006). These activities could be the signature of distributed neural cooperation required to achieve a task. The existence of distinct functional activities at distinct frequencies would be related to the existence of a multiplexing scheme enabling concomitant cognitive processes to participate in a given task.

Acknowledgments

We thank Antoine Ducorps and Frédéric Bergame for help with the data acquisition and computation. This experiment was supported by a grant from French ministry of research (ACI Neurosciences Intégratives et computationnelles) and the Agence Nationale de la Recherche (Projet Impression) to C. T. B. M. C. was supported by a grant from the Délégation Générale pour l'Armement (DGA).

Reprint requests should be sent to Maximilien Chaumon, Laboratoire de Neurosciences Cognitives et Imagerie Cérébrale, LENA CNRS UP640, 47 Bd de l'Hôpital, 75651 Paris Cedex 13, France, or via e-mail: maximilien.chaumon@gmail.com.

REFERENCES

Abbott, L. F., & Nelson, S. B. (2000). Synaptic plasticity: Taming the beast. *Nature Neuroscience, 3 (Suppl.),* 1178–1183.

Ahissar, M., & Hochstein, S. (2004). The reverse hierarchy theory of visual perceptual learning. *Trends in Cognitive Sciences, 8,* 457–464.

Bar, M. (2004). Visual objects in context. *Nature Reviews Neuroscience, 5,* 617–629.

Bar, M., Kassam, K. S., Ghuman, A. S., Boshyan, J., Schmidt, A. M., Dale, A. M., et al. (2006). Top–down facilitation of visual recognition. *Proceedings of the National Academy of Sciences, U.S.A., 103,* 449–454.

Bauer, E. P., Paz, R., & Pare, D. (2007). Gamma oscillations coordinate amygdalo-rhinal interactions during learning. *Journal of Neuroscience, 27,* 9369–9379.

Bi, G.-Q., & Poo, M.-M. (1998). Synaptic modifications in cultured hippocampal neurons: Dependence on spike timing, synaptic strength, and postsynaptic cell type. *Journal of Neuroscience, 18,* 10464–10472.

Bi, G.-Q., & Rubin, J. (2005). Timing in synaptic plasticity: From detection to integration. *Trends in Neurosciences, 28,* 222–228.

Bragin, A., Jando, G., Nadasdy, Z., Hetke, J., Wise, K., & Buzsaki, G. (1995). Gamma (40–100 Hz) oscillation in the hippocampus of the behaving rat. *Journal of Neuroscience, 15,* 47–60.

Brainard, D. H. (1997). The Psychophysics Toolbox. *Spatial Vision, 10,* 433–436.

Burgess, N., Maguire, E. A., & O'Keefe, J. (2002). The human hippocampus and spatial and episodic memory. *Neuron, 35,* 625–641.

Chaumon, M., Drouet, V., & Tallon-Baudry, C. (2008). Unconscious associative memory affects visual processing before 100 ms. *Journal of Vision, 8,* 1–10.

Chun, M. M., & Jiang, Y. (1998). Contextual cueing: Implicit learning and memory of visual context guides spatial attention. *Cognitive Psychology, 36,* 28–71.

Chun, M. M., & Jiang, Y. (2003). Implicit, long-term spatial contextual memory. *Journal of Experimental Psychology: Learning, Memory, and Cognition, 29,* 224–234.

Csicsvari, J., Jamieson, B., Wise, K. D., & Buzsaki, G. (2003). Mechanisms of gamma oscillations in the hippocampus of the behaving rat. *Neuron, 37,* 311–322.

Dan, Y., & Poo, M.-M. (2004). Spike timing-dependent plasticity of neural circuits. *Neuron, 44,* 23–30.

Desimone, R. (1996). Neural mechanisms for visual memory and their role in attention. *Proceedings of the National Academy of Sciences, U.S.A., 93,* 13494–13499.

Fell, J., Klaver, P., Lehnertz, K., Grunwald, T., Schaller, C., Elger, C. E., et al. (2001). Human memory formation is accompanied by rhinal–hippocampal coupling and decoupling. *Nature Neuroscience, 4,* 1259–1264.

Fiebach, C. J., Gruber, T., & Supp, G. G. (2005). Neuronal mechanisms of repetition priming in occipitotemporal cortex: Spatiotemporal evidence from functional magnetic resonance imaging and electroencephalography. *Journal of Neuroscience, 25,* 3414–3422.

Fries, P., Reynolds, J. H., Rorie, A. E., & Desimone, R. (2001). Modulation of oscillatory neuronal synchronization by selective visual attention. *Science, 291,* 1560–1563.

Gonzalez Andino, S. L., Michel, C. M., Thut, G., Landis, T., & Grave de Peralta, R. (2005). Prediction of response speed by anticipatory high-frequency (gamma band) oscillations in the human brain. *Human Brain Mapping, 24,* 50–58.

Gratton, G., Coles, M. G., & Donchin, E. (1983). A new method for off-line removal of ocular artifact. *Electroencephalography and Clinical Neurophysiology, 55,* 468–484.

Greene, A. J., Gross, W. L., Elsinger, C. L., & Rao, S. M. (2007). Hippocampal differentiation without recognition: An fMRI analysis of the contextual cueing task. *Learning and Memory, 14,* 548–553.

Grill-Spector, K., Henson, R., & Martin, A. (2006). Repetition and the brain: Neural models of stimulus-specific effects. *Trends in Cognitive Sciences, 10,* 14–23.

Gruber, T., Keil, A., & Müller, M. M. (2001). Modulation of induced gamma band responses and phase synchrony in a paired associate learning task in the human EEG. *Neuroscience Letters, 316,* 29–32.

Gruber, T., & Müller, M. M. (2002). Effects of picture repetition on induced gamma band responses, evoked potentials, and phase synchrony in the human EEG. *Brain Research, Cognitive Brain Research, 13,* 377–392.

Gruber, T., & Müller, M. M. (2005). Oscillatory brain activity dissociates between associative stimulus content in a repetition priming task in the human EEG. *Cerebral Cortex, 15,* 109–116.

Gruber, T., & Müller, M. M. (2006). Oscillatory brain activity in the human EEG during indirect and direct memory tasks. *Brain Research, 1097,* 194–204.
Gruber, T., Müller, M. M., Keil, A., & Elbert, T. (1999). Selective visual–spatial attention alters induced gamma band responses in the human EEG. *Clinical Neurophysiology, 110,* 2074–2085.
Gruber, T., Trujillo-Barreto, N. J., Giabbiconi, C. M., Valdes-Sosa, P. A., & Müller, M. M. (2006). Brain electrical tomography (BET) analysis of induced gamma band responses during a simple object recognition task. *Neuroimage, 29,* 888–900.
Gruber, T., Tsivilis, D., Montaldi, D., & Müller, M. M. (2004). Induced gamma band responses: An early marker of memory encoding and retrieval. *NeuroReport, 15,* 1837–1841.
Hebb, D. O. (1949). *The organization of behavior: A neuropsychological theory* (2002 ed.). Mahwah, NJ: Erlbaum.
Herrmann, C. S., Munk, M. H., & Engel, A. K. (2004). Cognitive functions of gamma-band activity: Memory match and utilization. *Trends in Cognitive Sciences, 8,* 347–355.
Hochstein, S., & Ahissar, M. (2002). View from the top: Hierarchies and reverse hierarchies in the visual system. *Neuron, 36,* 791–804.
Hoogenboom, N., Schoffelen, J. M., Oostenveld, R., Parkes, L. M., & Fries, P. (2006). Localizing human visual gamma-band activity in frequency, time and space. *Neuroimage, 29,* 764–773.
Jensen, O., Kaiser, J., & Lachaux, J. P. (2007). Human gamma-frequency oscillations associated with attention and memory. *Trends in Neurosciences, 30,* 317–324.
Jiang, Y., Song, J., & Rigas, A. (2005). High-capacity spatial contextual memory. *Psychonomic Bulletin & Review, 12,* 524–529.
Kaiser, J., Buhler, M., & Lutzenberger, W. (2004). Magnetoencephalographic gamma-band responses to illusory triangles in humans. *Neuroimage, 23,* 551–560.
Kiebel, S. J., Tallon-Baudry, C., & Friston, K. J. (2005). Parametric analysis of oscillatory activity as measured with EEG/MEG. *Human Brain Mapping, 26,* 170–177.
Lachaux, J.-P., Rodriguez, E., Martinerie, J., & Varela, F. J. (1999). Measuring phase synchrony in brain signals. *Human Brain Mapping, 8,* 194–208.
Lau, H. C., & Passingham, R. E. (2007). Unconscious activation of the cognitive control system in the human prefrontal cortex. *Journal of Neuroscience, 27,* 5805–5811.
Markram, H., Lubke, J., Frotscher, M., & Sakmann, B. (1997). Regulation of synaptic efficacy by coincidence of postsynaptic APs and EPSPs. *Science, 275,* 213–215.
Melloni, L., Molina, C., Pena, M., Torres, D., Singer, W., & Rodriguez, E. (2007). Synchronization of neural activity across cortical areas correlates with conscious perception. *Journal of Neuroscience, 27,* 2858–2865.
Miller, E. K., & Cohen, J. D. (2001). An integrative theory of prefrontal cortex function. *Annual Review of Neuroscience, 24,* 167–202.
Miltner, W. H., Braun, C., Arnold, M., Witte, H., & Taub, E. (1999). Coherence of gamma-band EEG activity as a basis for associative learning. *Nature, 397,* 434–436.
Montgomery, S. M., & Buzsaki, G. (2007). Gamma oscillations dynamically couple hippocampal CA3 and CA1 regions during memory task performance. *Proceedings of the National Academy of Sciences, U.S.A., 104,* 14495–14500.
Neumann, O., & Klotz, W. (1994). Motor responses to nonreportable, masked stimuli: Where is the limit of direct parameter specification? In C. Umiltà & M. Moscovitch (Eds.), *Conscious and nonconscious information processing* (Vol. XV, pp. 123–150). Cambridge, MA: MIT Press.
Oliva, A. (2005). Gist of the scene. In L. Itti, G. Rees, & J. K. Tsotsos (Eds.), *The encyclopedia of neurobiology of attention* (pp. 251–256). San Diego, CA: Elsevier.
Oliva, A., & Schyns, P. G. (1997). Coarse blobs or fine edges? Evidence that information diagnosticity changes the perception of complex visual stimuli. *Cognitive Psychology, 34,* 72–107.
Osipova, D., Takashima, A., Oostenveld, R., Fernandez, G., Maris, E., & Jensen, O. (2006). Theta and gamma oscillations predict encoding and retrieval of declarative memory. *Journal of Neuroscience, 26,* 7523–7531.
Rodriguez, R., Kallenbach, U., Singer, W., & Munk, M. H. J. (2004). Short- and long-term effects of cholinergic modulation on gamma oscillations and response synchronization in the visual cortex. *Journal of Neuroscience, 24,* 10369–10378.
Rose, M., Haider, H., & Büchel, C. (2005). Unconscious detection of implicit expectancies. *Journal of Cognitive Neuroscience, 17,* 918–927.
Ross, R. S., & Slotnick, S. D. (2008). The hippocampus is preferentially associated with memory for spatial context. *Journal of Cognitive Neuroscience, 20,* 432–446.
Schurger, A., Cowey, A., & Tallon-Baudry, C. (2006). Induced gamma-band oscillations correlate with awareness in hemianopic patient GY. *Neuropsychologia, 44,* 1796–1803.
Sederberg, P. B., Kahana, M. J., Howard, M. W., Donner, E. J., & Madsen, J. R. (2003). Theta and gamma oscillations during encoding predict subsequent recall. *Journal of Neuroscience, 23,* 10809–10814.
Sederberg, P. B., Schulze-Bonhage, A., Madsen, J. R., Bromfield, E. B., McCarthy, D. C., Brandt, A., et al. (2007). Hippocampal and neocortical gamma oscillations predict memory formation in humans. *Cerebral Cortex, 17,* 1190–1196.
Sejnowski, T. J., & Paulsen, O. (2006). Network oscillations: Emerging computational principles. *Journal of Neuroscience, 26,* 1673–1676.
Singer, W. (1995). Development and plasticity of cortical processing architectures. *Science, 270,* 758–764.
Singer, W. (1999). Time as coding space? *Current Opinion in Neurobiology, 9,* 189–194.
Smyth, A. C., & Shanks, D. R. (2008). Awareness in contextual cuing with extended and concurrent explicit tests. *Memory & Cognition, 36,* 403–415.
Stiefel, K. M., Tennigkeit, F., & Singer, W. (2005). Synaptic plasticity in the absence of backpropagating spikes of layer II inputs to layer V pyramidal cells in rat visual cortex. *European Journal of Neuroscience, 21,* 2605–2610.
Summerfield, C., & Mangels, J. A. (2006). Dissociable neural mechanisms for encoding predictable and unpredictable events. *Journal of Cognitive Neuroscience, 18,* 1120–1132.
Supp, G. G., Schlögl, A., Trujillo-Barreto, N., Müller, M. M., & Gruber, T. (2007). Directed cortical information flow during human object recognition: Analyzing induced EEG gamma-band responses in brain's source space. *PLoS ONE, 2,* e684.
Tallon-Baudry, C., & Bertrand, O. (1999). Oscillatory gamma activity in humans and its role in object representation. *Trends in Cognitive Sciences, 3,* 151–162.
Tallon-Baudry, C., Bertrand, O., Delpuech, C., & Pernier, J. (1997). Oscillatory gamma-band (30–70 Hz) activity induced by a visual search task in humans. *Journal of Neuroscience, 17,* 722–734.

Tallon-Baudry, C., Bertrand, O., Delpuech, C., & Pernier, J. (1996). Stimulus specificity of phase-locked and non-phase-locked 40 Hz visual responses in human. *Journal of Neuroscience, 16,* 4240–4249.

Tallon-Baudry, C., Bertrand, O., & Fischer, C. (2001). Oscillatory synchrony between human extrastriate areas during visual short-term memory maintenance. *Journal of Neuroscience, 21,* RC177.

VanRullen, R. (2003). Visual saliency and spike timing in the ventral visual pathway. *Journal of Physiology Paris, 97,* 365–377.

Vidal, J. R., Chaumon, M., O'Regan, J. K., & Tallon-Baudry, C. (2006). Visual grouping and the focusing of attention induce gamma-band oscillations at different frequencies in human magnetoencephalogram signals. *Journal of Cognitive Neuroscience, 18,* 1850–1862.

Wespatat, V., Tennigkeit, F., & Singer, W. (2004). Phase sensitivity of synaptic modifications in oscillating cells of rat visual cortex. *Journal of Neuroscience, 24,* 9067–9075.

Wiggs, C. L., & Martin, A. (1998). Properties and mechanisms of perceptual priming. *Current Opinion in Neurobiology, 8,* 227–233.

Wyart, V., & Tallon-Baudry, C. (2008). Neural dissociation between visual awareness and spatial attention. *Journal of Neuroscience, 28,* 2667–2679.

This article has been cited by:

1. Olaleke O. Oke, Andor Magony, Himashi Anver, Peter D. Ward, Premysl Jiruska, John G. R. Jefferys, Martin Vreugdenhil. 2010. High-frequency gamma oscillations coexist with low-frequency gamma oscillations in the rat visual cortex in vitro. *European Journal of Neuroscience* **31**:8, 1435-1445. [CrossRef]
2. Karim Jerbi, Tomás Ossandón, Carlos M. Hamamé, S. Senova, Sarang S. Dalal, Julien Jung, Lorella Minotti, Olivier Bertrand, Alain Berthoz, Philippe Kahane, Jean-Philippe Lachaux. 2009. Task-related gamma-band dynamics from an intracerebral perspective: Review and implications for surface EEG and MEG. *Human Brain Mapping* **30**:6, 1758-1771. [CrossRef]